Synthesis and Characterization of Sterically Hindered Group IV Metallocenes

Brian J. Grimmond, Joyce Y. Corey,* and Nigam P. Rath

University of Missouri−St. Louis, 8001 Natural Bridge Road, St. Louis, Missouri 63121

Received October 15, 1998

Three new C_2 symmetric heteroannular dialkyl substituted group IV metallocene dichlorides $(Cp^R)_2MCl_2$ [$Cp^R = C_5H_4C(Me)_2CHMe_2$; M = Zr (**2**), Hf (**3**), Ti (**4**)] were synthesized as potential catalytic precursors for the dehydropolymerization of silanes to polysilanes. The hindered complexes were generated in fair yield by reaction of 2 equiv of the alkyllithium reagent Cp^RLi (**1**) and the corresponding metal halide, MCl_4·2THF for **2** and **3** and MCl_3·3THF for **4**. Crystal structures for compounds **2**−**4** were obtained and established a pseudotrans configuration of the ancillary ligands in the solid state. The structural features adopted by these compounds to accommodate the large substituents are described with comparisons to known metallocenes. Monoalkyl-substituted metallocenes $Cp(Cp^R)MCl_2$, M = Ti (**5**), Zr (**6**), were also synthesized from **1** and the corresponding monocylopentadienyltrihalide species $CpMCl_3$. Characterization of **2**−**6** by various NMR techniques in conjunction with solid-state analysis of **2**, **3**, and **4** permitted interpretation of an interligand mechanism for the observed NOE signals involving the *distal* protons of the substituted cyclopentadienyl ligand and portions of the alkyl cyclopentadienyl substituent.

Introduction

Polysilanes are a relatively new series of inorganic polymers consisting of a Si−Si covalent network with unique σ-bond delocalization properties. Consequently, the polymers have potential in various technical applications[1−4] prompting the development of several synthetic techniques,[5−7] which include catalytic dehydropolymerization of primary and secondary silanes with group IV metallocenes.[8−10]

As the mechanistic complexities of this procedure are uncovered,[11−14] systematic alterations of the metallocene structure introduce new catalyst characteristics which can then be employed to test the understanding of such catalytic events. Namely, substitution of the ancillary cyclopentadienyl rings would be expected to modulate the reactivity of the metal site via steric and electronic means. Rational modification of the metal environment in such a manner is expected to have consequences in the propagation of the polysilane, and by assaying the characteristics of the polymer obtained from a range of substituted metallocenes, the requirements associated with an efficient catalyst should be derived, in principle, by correlation to the architecture of the catalyst used. With this goal in mind, a series of group IV metallocene dichlorides [$(Cp^R)_2MCl_2$ and $Cp(Cp^R)MCl_2$] have been synthesized (Figure 1) and the influence of substituent effects on polyphenylsilane formation has been investigated. The purpose of this

(1) (a) Miller, R. D.; Michl, J. *Chem. Rev.* **1989**, *89*, 1359. (b) Tilley, T. D. *Acc. Chem. Res.* **1993**, *26*, 22. (c) Manners, I. *Angew. Chem., Int. Ed. Engl.* **1996**, *35*, 1602.

(2) Kanemitsu, K.; Suzuki, K.; Masumoto, T.; Komatsu, K.; Sato, K.; Kyushin, S.; Matsumoto, H. *Solid State Commun.* **1993**, *86*, 545.

(3) (a) Scarlete, M.; Butler, I. S.; Harrod, *J. Chem. Mater.* **1995**, *7*, 1214. (b) West, R. *J. Organomet. Chem.* **1986**, *300*, 327.

(4) Solangi, A.; Chaudry, M. *J. Mater. Res.* **1992**, *7*, 247.

(5) (a) Wesson, J. P.; Williams T. C. *J. Polym. Sci. Polym. Chem.* **1980**, *18*, 959. (b) Trujillo, R. E. *J. Organomet. Chem.* **1980**, *198*, C27. (c) Devaux, J.; Sledz, F.; Giral, L.; Naarmann, H. *Eur. Polym. J.* **1989**, *25*, 263. (d) Jones, R. G.; Benfield, R. E.; Evans, P. J.; Holder, S. J.; Locke, J. A. M. *J. Organomet. Chem.* **1996**, *521*, 171. (e) Harrah, L. A.; Zeigler, J. M. *Ibid.* **1995**, *14*, 2506.

(6) (a) Price, G. *J. Chem. Soc., Chem. Commun.* **1992**, 1209.

(7) (a) Bianconi, P. A.; Weidman, *J. Am. Chem. Soc.* **1988**, *110*, 2342. (b) Shono, T.; Kashimura, S. Ishifune, M.; Nishida, R. *J. Chem. Soc., Chem. Commun.* **1990**, 1160. (c) Bordeau, M.; Biran, C.; Leger-Lambert, M.-P.; Dunogues. *Ibid.* **1991**, 1476. (d) Vermeulen, L. A.; Huang, K. *Ibid.* **1998**, 247. (e) Kimata, Y.; Suzuki, H.; Satoh, S.; Kuriyama, A. *Organometallics* **1995**, *14*, 2506.

(8) (a) Fontaine, G.-G.; Kadkhodazadeh, T.; Zargarian, D. *J. Chem. Soc., Chem. Commun.* **1998**, 1253. (b) Chauhan, B. P. S.; Shimizu, T.; Tanaka, M. *Chem. Lett.* **1997**, 785. (c) Peulecke, N.; Thomas, D.; Baumann, W.; Fischer, C.; Rosenthal, U. *Tetrahedron. Lett.* **1997**, *38*, 6655. (d) Jutzi, P.; Redeker, T.; Neumann, B.; Stammler, H.-G. *Chem. Ber.* **1996**, *129*, 1509. (e) Jutzi, P.; Redeker, T.; Neumann, B.; Stammler, H.-G. *Organometallics* **1996**, *15*, 4153.

(9) Aitken, C.; Harrod, J. F.; Henique, J.; Samuel, E. *J. Organomet. Chem.* **1985**, *279*, C11.

(10) (a) Corey, J. Y.; Zhu, X. H.; Bedard, T. C.; Lange, L. D. *Organometallics* **1991**, *10*, 924. (b) Corey, J. Y.; Zhu, X. H. *J. Organomet. Chem.* **1992**, *439*, 1. (c) Corey, J. Y. Zhu, X. H. *Organometallics* **1992**, *11*, 1672. (d) Corey, J. Y.; Huhmann, J. L.; Zhu, X. H. *Organometallics* **1993**, *12*, 1121. (e) Shaltout, R. M.; Corey, J. Y. *Tetrahedron* **1995**, *51*, 4309. (f) Huhmann, J. L.; Corey, J. Y.; Rath, N. P. *J. Organomet. Chem.* **1997**, *533*, 51.

(11) Woo, H. G.; Walzer, J. F.; Tilley, T. D. *J. Am. Chem. Soc.* **1992**, *114*, 7047.

(12) For a related σ-bond metathesis, see: (a) Thompson, M. E.; Baxter, S. M.; Bulls, A. R.; Burger, B. J.; Nolan, M. C.; Santarsiero, B. D.; Schaefer, W. P.; Bercaw, J. E. *J. Am. Chem. Soc.* **1987**, *109*, 203. For σ-bond metathesis of silanes, see: (b) Woo, H. G.; Tilley, T. D. *J. Am. Chem. Soc.* **1989**, *111*, 3757. (c) Woo, H. G.; Tilley, T. D. *Polym. Prepr.* (*Am. Chem. Soc., Div. Polym. Chem.*) **1990**, *31*, 228.

(13) (a) Jia, L.; Yang, X.; Sterm, C. L.; Marks, T. J. *Organometallics* **1997**, *16*, 842. (b) Bochmann, M. *J. Chem. Soc., Dalton Trans.* **1996**, 255. (c) Britzinger, H. H.; Leclerc, M. K. *J. Am. Chem. Soc.* **1996**, *118*, 9024. (d) Wu, Z.; Jordan, R. F.; Peterson, J. L. *Ibid.* **1995**, *117*, 5867. (e) Giardello, M. A.; Eisen, M. S.; Stern, C. L. Marks, T. J. *Ibid.* **1995**, *117*, 12114. (f) Bochmann, M.; Lancaster, S. J. *Angew. Chem., Int. Ed. Engl.* **1994**, *33*, 1635. (g) Pellechia, C.; Grassi, A.; Zambelli, A. *Organometallics* **1994**, *13*, 298. (h) Jordan, R. F. *J. Chem. Ed.* **1988**, *65*, 285.

(14) (a) Dioumaev, V. K.; Harrod, J. F. *Organometallics* **1997**, *16*, 2798. (b) Dioumaev, V. K. Harrod, J. F. *Organometallics* **1996**, *15*, 3859.

10.1021/om9808615 CCC: $18.00
Publication on Web 01/15/1999

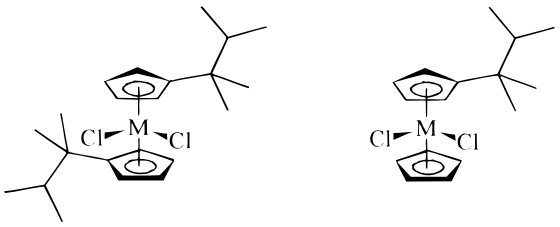

$(Cp^R)_2MCl_2$ $Cp(Cp^R)MCl_2$

Figure 1. Bisalkyl-substituted and monoalkyl-substituted metallocene dichlorides.

paper is to describe the synthesis and in-depth structural characteristics of these precatalysts; a subsequent paper will describe the use of these precatalysts in the condensation of $PhSiH_3$.

Experimental Section

General Comments. All reactions were run under an atmosphere of dry nitrogen using Schlenk glassware or a glovebox, unless otherwise stated. Reaction vessels were flame dried under a stream of nitrogen, and anhydrous solvents were transferred by oven-dried syringes or cannula. Tetrahydrofuran was distilled from calcium hydride and then from sodium benzophenone ketyl; ether was distilled from sodium benzophenone ketyl. Toluene and hexanes were distilled from calcium hydride; dichloromethane was washed with sulfuric acid, neutralized, and distilled from calcium hydride.

Microanalyses were performed by Atlantic Microlab, Inc., Norcross, GA. High-resolution mass spectral data (FAB) were collected by the Washington University Resource for Biomedical and Bio-organic Mass Spectrometry.

Proton and carbon-13 (^1H, ^{13}C) nuclear magnetic resonance spectra were recorded using either a Varian Unity + 300 equipped with a multi nuclear probe or a Bruker ARX500 equipped with a broad band or inverse probe. Two-dimensional studies were performed using a Bruker ARX500. Unless otherwise stated, spectra were recorded in $CDCl_3$ and referenced internally to residual solvent peaks ($CHCl_3$) or to TMS. Chemical shifts (δ) are reported in ppm and coupling constants (J) in hertz. ^1H NMR used for accurate determination of signal ratios were run with a delay of 0.5−1.0 s to minimize the effects of differential relaxation periods.

$C_5H_4CMeC(H)Me_2$,[15] $CpTiCl_3$,[16] $CpZrCl_3$·2THF,[17] and $TiCl_3$·3THF[18] were prepared according to literature procedures.

Crystallographic Structure Determinations. Crystals of appropriate dimensions were mounted on glass fibers in random orientation. Preliminary examination and data collection were performed using a Bruker SMART charge coupled device (CCD) detector system single-crystal X-ray diffractometer using graphite-monochromated Mo Kα radiation (λ = 0.710 73 Å) equipped with a sealed tube X-ray source. Preliminary unit cell constants were determined with a set of 45 narrow frames (0.3° in ω) and counting time of 15 s/frame at a crystal detector distance of 4.9 cm. The double-pass method of scanning was used to exclude any noise. The collected frames were integrated using orientation matrixes determined from the narrow frame scans. The SMART software package (Bruker Analytical X-ray, Madison, WI, 1997) was used for data collection, and the SAINT package (Bruker Analytical X-ray, Madison, WI, 1997) was used for frame integration. Analysis of the integrated data did not show any decay. Final cell constants were determined by a global refinement of the *xyz* centroids of 8192 reflections. Absorption correction was applied to the data using equivalent reflections (SADABS). Crystal data and intensity data collection parameters are listed in Table 1. Structure solution and refinement were carried out using the SHELXTL-PLUS software package (Scheldrick, G. M., BrukerAnalytical X-Ray Division, Madison, WI, 1997). The structures were solved by direct methods and refined successfully in the space group *C*2/*c*. Full matrix least squares refinement was carried out minimizing $\sum w(F_o^2 - F_c^2)^2$. The nonhydrogen atoms were refined anisotropically to convergence. All the hydrogen atoms were refined freely. Structure refinement parameters, atomic coordinates for the non-hydrogen atoms, and selected geometrical parameters are submitted in the Supporting Information. A complete list of positional and isotropic displacement coeffiecients for hydrogen atoms, anisotropic displacement for the non-hydrogen atoms, and a complete list of geometrical parameters are submitted in the Supporting Information.

Calculated and observed structure factors (F_o/F_c tables) can be provided in electronic media or hard copy format as necessary.

Synthesis of $C_5H_4C(Me)_2C(H)Me_2$·Li (1). A sample of $C_5H_4CMe_2C(H)Me_2$ (5.0 g, 37.3 mmol) was dissolved in ether (50 mL) to give a yellow solution, which was cooled to 0 °C. An aliquot of MeLi (26.6 mL 37.3 mmol) was added dropwise to the solution over 10 min, resulting in precipitation of a white solid with concomitant discharge of the yellow color. Stirring for 12 h with gradual warming to ambient temperature gave a colorless solution and a white precipitate, which was filtered, washed with ether (2 × 50 mL), and dried in vacuo to yield **1** as a white powder (4.59 g, 79% yield).

Synthesis of $[C_5H_4C(Me)_2C(H)Me_2]_2ZrCl_2$ (2). A Schlenk tube was charged with **1** (1.00 g, 6.4 mmol) and $ZrCl_4$ (0.75 g, 3.2 mmol) and cooled to −78 °C. Ether (20 mL) was introduced with shaking of the reaction vessel. The reaction mixture was stirred for 12 h to give a white suspension and an orange solution. The solid was filtered, washed with ether (2 × 10 mL), and dried in vacuo. CH_2Cl_2 (20 mL) was added and the mixture stirred for 20 min. Filtration of the pale yellow solution through Celite and storage at 0 °C for 12 h gave **2** as colorless needles (0.35 g, 24% yield). ^1H NMR (500 MHz, $CDCl_3$, 303 K): δ 6.40 (t, 4 H, J = 2.7 Hz) Cp*H proximal*, δ 6.30 ppm (t, 4 H, J = 2.7 Hz) Cp*H distal*, δ 1.57 (spt, 2 H, ^3J = 6.8 Hz) C*H*(Me)$_2$, δ 1.35 (s, 12 H) C(C*H*$_3$)$_2$, δ 0.68 (d, 12 H, ^3J = 6.8 Hz) CH(C*H*$_3$)$_2$. ^{13}C {^1H}NMR (500 MHz, $CDCl_3$, 303 K): δ 143.16 Cp *ipso*, δ 116.91 Cp *proximal*, δ 112.44 Cp *distal*, δ 41.72 *C*H(Me)$_2$, δ 39.56 *C*(Me)$_2$, δ 23.68 C(*C*H$_3$)$_2$, δ 18.12 CH(*C*H$_3$)$_2$. Anal. Calcd for $C_{22}H_{34}ZrCl_2$: C, 57.36; H, 7.44. Found: C, 57.31; H, 7.24.

Synthesis of $[C_5H_4C(Me)_2C(H)Me_2]_2HfCl_2$ (3). In a manner similar to that used to synthesize **2**, compound **1** (0.80 g, 5.0 mmol) and $HfCl_4$ (0.80 g 2.5 mmol) gave **3** as colorless needles (0.27 g, 20% yield). ^1H NMR (500 MHz, $CDCl_3$, 303 K): δ 6.29 (t, 4 H, J = 2.7 Hz) Cp*H proximal*, δ 6.22 (t, 4 H, J = 2.7 Hz) Cp*H distal*, δ 1.53 (spt, 2 H, ^3J = 6.8 Hz) C*H*(Me)$_2$, δ 1.35 (s, 12 H) C(C*H*$_3$)$_2$, δ 0.64 (d, 12 H, ^3J = 6.8 Hz) CH(C*H*$_3$)$_2$. ^{13}C {^1H}NMR (500 MHz, $CDCl_3$, 303 K): δ 141.0 Cp − *ipso*, δ 115.4 Cp *proximal*, δ 111.2 Cp *distal*, δ 42.0 *C*H(Me)$_2$, δ 39.4 *C*(Me)$_2$, δ 23.7 C(*C*H$_3$)$_2$, δ 18.2. CH(*C*H$_3$)$_2$. Anal. Calcd for $C_{22}H_{34}HfCl_2$: C, 48.23; H, 6.25. Found: C, 47.99; H, 6.26.

Synthesis of $[C_5H_4C(Me)_2C(H)Me_2]_2TiCl_2$ (4). A Schlenk tube was charged with **1** (1.00 g, 6.4 mmol) and $TiCl_3$·3THF (1.20 g, 3.2 mmol) and cooled to −78 °C. THF (40 mL) was introduced, and the reaction mixture was stirred for 12 h and gradually warmed to room temperature. The resultant dark blue-black solution was heated at 70 °C for 30 min and then allowed to cool to room temperature. The solvent was removed in vacuo to yield a dark brown residue, which was converted to a slurry by addition of pentanes (20 mL) and stirring. The

(15) Stone, K. J.; Little, R. D. *J. Org. Chem*. **1984**, 11, *1849*.
(16) Cardoso, A. M.; Clark, R. J. H.; Moorhouse, S. J. *J. Chem. Commun., Dalton Trans.* **1980**, 1156.
(17) (a) Lund, E. C.; Livinghouse, T. *Organometallics* **1990**, *9*, 2426. (b) Erker, G.; Berg, K.; Treschanke, L.; Engel, K. *Inorg. Chem*. **1982**, *21*, 1277.
(18) Manzer, L. E. *Inorg. Synth*. **1982**, *21*, 135.

Table 1. Crystal Data and Data Collection Parameters of 2, 3, and 4

	$C_{22}H_{34}ZrCl_2$	$C_{22}H_{34}HfCl_2$	$C_{22}H_{34}TiCl_2$
fw	460.62	547.88	417.29
temp	213(2) K	223(2) K	223(2) K
wavelength	0.710 73 Å	0.710 73 Å	0.710 73 Å
cryst syst	monoclinic	monoclinic	monoclinic
space group	*C*2/*c*	*C*2/*c*	*C*2/*c*
unit cell dimen	$a = 18.4089(2)$ Å, $\alpha = 90°$ $b = 6.6504(1)$ Å, $\beta = 99.950°$ $c = 18.2915(1)$ Å, $\gamma = 90°$	$a = 18.3679(2)$ Å, $\alpha = 90°$ $b = 6.6420(1)$ Å, $\beta = 100.464(1)°$ $c = 18.2908(1)$ Å, $\gamma = 90°$	$a = 18.2957(3)$ Å, $\alpha = 90°$ $b = 6.5568(2)$ Å, $\beta = 100.202(1)°$ $c = 18.1323(5)$ Å, $\gamma = 90°$
volume	2205.68(4) Å^3	2194.36(4) Å^3	2140.78(9) Å^3
Z	8	4	4
density (calcd)	1.387 Mg/m^3	1.658 Mg/m^3	1.295 Mg/m^3
abs coeff	0.744 mm^{-1}	5.000 mm^{-1}	0.652 mm^{-1}
F(000)	960	1088	888
cryst size	0.17 × 0.04 × 0.02 mm^3	0.38 × 0.20 × 0.20 mm^3	0.40 × 0.10 × 0.02 mm^3
θ range for data collection	2.25−29.78°	2.26−29.87°	2.26−25.00°
index ranges	$-25 < h < 24$, $-9 < k < 8$, $-24 < l < 24$	$-25 < h < 24$, $0 < k < 9$, $0 < l < 24$	$-22 < h < 22$, $0 < k < 8$, $0 < l < 22$
no. of reflns collected	14720	24058	8840
no. of ind reflns	2975 [R(int) = 0.0768]	3021 [R(int) = 0.041]	1885 [R(int) = 0.1]
abs corr	empirical	empirical, sadabs	empirical
max. and min. transmission	0.36 and 0.69	0.91 and 0.53	0.82 and 0.62
refinement method	full matrix least-squares on F^2	full matrix least-squares on F^2	full matrix least-squares on F^2
no. of data/restraints/params	2975/0/182	3018/0/ 183	1863/0/182
goodness of fit on F^2	0.974	1.127	1.036
final R indices [$I2\sigma(I)$]	R1 = 0.0368, wR2 = 0.0708	R1 = 0.0153, wR2 = 0.0308	R1 = 0.0511, wR2 = 0.0895
R indices (all data)	R1 = 0.0587, wR2 = 0.0763	R1 = 0.0165, wR2 = 0.0328	R1 = 0.1013, wR2 = 0.1101
largest diff peak and hole	0.395 and −0.814 e Å^{-3}	0.706 and −0.989 e Å^{-3}	0.283 and −0.315 e Å^{-3}

volatiles were removed in vacuo, and the process was repeated to afford a red-brown solid, which was then redissolved in CH_2Cl_2 (60 mL). Washing the brown solution with 4 M HCl (2 × 10 mL) resulted in formation of a bright red solution and precipitation of a red solid. The mixture was extracted with H_2O (3 × 10 mL) and the organic layer separated. The aqueous layer was washed with CH_2Cl_2 (2 × 20 mL), and the combined organic extracts were then dried over anhydrous Na_2SO_4. Reduction of the volume to 30 mL followed by storage at 0 °C gave **4** as red needlelike crystals (0.62 g, 46% yield). ^{1}H NMR (500 MHz, $CDCl_3$, 303 K): δ 6.51 (t, 4 H, J = 2.6 Hz) Cp*H proximal*, δ 6.45 (t, 4 H, J = 2.6 Hz) Cp*H distal*, δ 1.54 (spt, 2 H, ^3J = 6.9 Hz) C*H*(Me)$_2$, δ 1.33 (s, 12 H) C(C*H*$_3$)$_2$, δ 0.70 (d, 12 H, ^3J = 6.9 Hz) CH(C*H*$_3$)$_2$. ^{13}C {^{1}H}NMR (500 MHz, $CDCl_3$, 303 K): δ 148.57 Cp *ipso*, δ 120.87 Cp *proximal*, δ 117.31 Cp *distal*, δ 42.04 *C*H(Me)$_2$, δ 40.49 *C*(Me)$_2$, δ 23.20 C(*C*H$_3$)$_2$, δ 18.13 CH(*C*H$_3$)$_2$. Anal. Calcd for $C_{22}H_{34}TiCl_2$: C, 63.32; H, 8.21. Found: C, 61.56; H, 7.66. A sample was recrystallized from CH_2Cl_2/hexanes (1:1) at −50 °C and the resulting precipitate sublimed (160 °C, 1 mTorr) to give a fine red powder. Anal. Calcd for $C_{22}H_{34}TiCl_2$: C, 63.32; H, 8.21. Found: C, 61.26; H, 7.95. No further purification attempts were made. MS−FAB: *m*/*z* 381 [M$^+$ − Cl]. HRMS (FAB): *m*/*z* calcd for $C_{22}H_{34}TiCl$ 381.1829, obsd 381.1813.

Synthesis of $C_5H_4[C_5H_4C(Me)_2C(H)Me_2]ZrCl_2$ (5). A Schlenk tube was charged with **1** (0.39 g, 2.5 mmol) and $CpZrCl_3$·2THF (1.00 g, 2.5 mmol) in a glovebox and transferred to a Schlenk line. On addition of Et_2O (20 mL) the reaction mixture was cooled to − 78 °C, and the resulting suspension was stirred for 12 h with gradual warming to room temperature to provide an orange solution and a colorless precipitate. The volatiles were removed in vacuo, and the residue was washed with pentanes (2 × 5 mL) and then redried in vacuo to give crude **5** as an off-white solid. Compound **5** was dissolved in CH_2Cl_2 (50 mL) and filtered through Celite, and the volume was reduced to ∼15 mL. Storage at −78 °C precipitated colorless microcrystals over 48 h. Filtration of the colorless solid followed by drying in vacuo afforded **5** as a colorless powder (0.46 g, 49% yield). ^{1}H NMR (500 MHz, $CDCl_3$, 303 K): δ 6.48 (s, 5 H) Cp*H*, δ 6.43 (t, 2 H, J = 2.6 Hz) Cp*H distal*, δ 6.36 (t, 2 H, J = 2.6 Hz) Cp*H proximal*, δ 1.56 (spt, 6 H, ^3J = 6.8 Hz) C*H*(Me)$_2$, δ 1.33 (s, 6 H) C(C*H*$_3$)$_2$, δ 0.65 (d, 6 H, ^3J = 6.8 Hz) CH(C*H*$_3$)$_2$. ^{13}C {^{1}H}NMR (500 MHz, $CDCl_3$, 303 K): δ 143.89 ppm Cp *ipso*, δ 116.14 *C*$_5$H$_4$, δ 116.25 *C*$_5$H$_5$, δ 113.34 *C*$_5$H$_4$, δ 41.7 *C*H(Me)$_2$, δ 39.50 ppm *C*(Me)$_2$, δ 23.76 C(*C*H$_3$)$_2$, δ 18.11 CH(*C*H$_3$)$_2$. Anal. Calcd for $C_{16}H_{22}ZrCl_2$: C, 51.05; H, 5.89. Found: C, 50.34; H, 5.81.

Synthesis of $C_5H_4[C_5H_4C(Me)_2C(H)Me_2]TiCl_2$ (6). A Schlenk tube was charged with **1** (0.40 g, 2.5 mmol) and $CpTiCl_3$ (0.55 g, 2.5 mmol) in a glovebox and transferred to a Schlenk line. On addition of Et_2O (20 mL) the reaction mixture was cooled to −78 °C and the resultant suspension stirred for 12 h with gradual warming to room temperature to provide a red solution and a precipitate. The volatiles were removed in vacuo, and the residue was washed with pentanes (2 × 5 mL), then dried in vacuo to give crude **6** as a red solid. Soxhlet extraction of crude **6** with CH_2Cl_2 (70 mL) over 12 h afforded a red solution, which was reduced in volume to ∼15 mL and stored at −50 °C. Precipitation of a red solid was observed over 48 h, at which point the solid was filtered and recrystallized from CH_2Cl_2/pentanes (1:2) to provide **6** as red microcrystals, which were dried in vacuo (0.33 g, 36% yield). ^{1}H NMR (500 MHz, $CDCl_3$, 303 K): δ 6.60 (t, 2 H, J = 2.6 Hz) Cp*H distal*, δ 6.54 (s, 5 H) Cp*H*, δ 6.50 (t, 2 H, J = 2.6 Hz) Cp*H proximal*, δ 1.56 (spt, 1 H, ^3J = 6.8 Hz) C*H*(Me)$_2$, δ 1.33 (s, 6 H) C(C*H*$_3$)$_2$, δ 0.65 (d, 6 H, ^3J = 6.8 Hz) CH(C*H*$_3$)$_2$. ^{13}C {^{1}H}NMR (500 MHz, $CDCl_3$, 303 K): δ 149.07 Cp *ipso*, δ 120.38 *C*$_5$H$_5$, δ 120.15 *C*$_5$H$_4$ *distal*, δ 118.68 *C*$_5$H$_4$ *proximal*, δ 41.95 *C*H(Me)$_2$, δ 40.48 ppm *C*(Me)$_2$, δ 23.32 C(*C*H$_3$)$_2$, δ 18.15 CH(*C*H$_3$)$_2$. On exposure to air, the hemihydrate of **6** is produced, displaying an additional resonance in the ^{1}H NMR δ = 1.54 (1 H). Anal. Calcd for $C_{16}H_{21}TiCl_2$·0.5(H_2O): C, 56.17; H, 6.78. Found: C, 55.78; H, 6.70.

Results and Discussion

Metallocene Synthesis. Fulvenes are subject to attack from nucleophiles such as lithium reagents at the positively polarized exo carbon. Synthesis of the fulvene $C_5H_4CMeC(H)Me_2$ by literature procedures followed by addition of 1 equiv of MeLi in Et_2O at 0 °C

Scheme 1

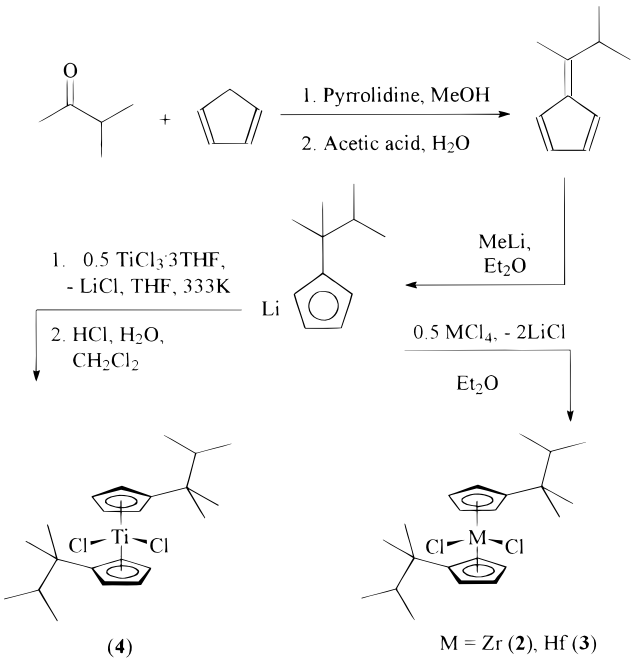

effects the precipitation of the cyclopentadienyllithium salt (**1**) in excellent yield as an air and moisture sensitive colorless powder which can be stored under an inert atmosphere.[19]

The heteroannular disubstituted metallocenes $[C_5H_4C(Me)_2C(H)Me_2]_2MCl_2$ (M = Zr [**2**], Hf [**3**]) were generated in fair yields by salt metathesis reactions of 2 equiv of **1** with $ZrCl_4$ and $HfCl_4$ in Et_2O. Filtration of the crude product, followed by isolation from lithium chloride by CH_2Cl_2 Soxhlet extraction and cooling to 0 °C, afforded analytically pure samples of the bent metallocene dichlorides as moderately air and moisture stable colorless needles (Scheme 1). However, in the synthesis of the titanium congener, a similar methodology using $TiCl_4$ or $TiCl_4$·2THF failed to cleanly produce the target compound due to facile reduction of the Ti[IV] center to Ti[III] by the lithium salt **1**. Modification of the salt elimination protocol, using $TiCl_3$·3THF in THF at 60 °C followed by aqueous oxidative HCl workup of the Ti[III] to Ti[IV] in CH_2Cl_2, drying over Na_2SO_4, and Celite filtration provided the product $[C_5H_4C(Me)_2C(H)Me_2]_2TiCl_2$ (**4**) as red needles on cooling to 0 °C (Scheme 1).[20] A single recrystallization in CH_2Cl_2 offered **4** as moderately air and moisture stable red needles. Although solid-state analysis of these needles indicated pure **4**, the C, H analysis of **4** proved low. Further purification by recrystallization and sublimation failed to provide a sample that gave satisfactory analysis. The C_2 symmetric heteroannular disubstituted compounds $(Cp^R)_2MCl_2$ **2**, **3**, and **4** were characterized by various NMR techniques, in addition to single-crystal X-ray diffraction.

Additionally, the monosubstituted bent metallocene dichlorides $C_5H_4[C_5H_4C(Me)_2C(H)Me_2]ZrCl_2$ (**5**) and $C_5H_4[C_5H_4C(Me)_2C(H)Me_2]TiCl_2$ (**6**) were also synthesized by a salt elimination approach similar to that used for **2** and **3** (Scheme 2). The compounds were purified by recrystallization from CH_2Cl_2/pentanes; however, the hygroscopic titanium analogue rapidly converted to the hemihydrate on exposure to air as established by ^1H NMR and elemental analysis.

Scheme 2

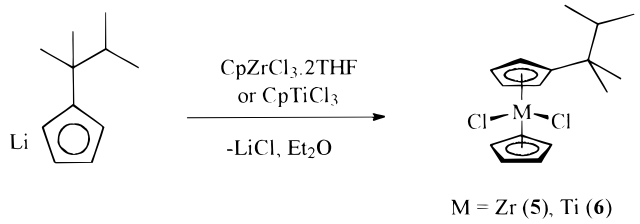

NMR Studies of Heteroannular Alkyl Disubstituted Metallocenes $(Cp^R)_2MCl_2$. The ^1H NMR spectra of **2**, **3**, and **4** displayed two pseudotriplets (δ 6.45 and 6.22 ppm) in the cyclopentadienyl region representing the second-order AA′BB′ spin system associated with *proximal* and *distal* protons of the substituted ring (Figure 2). The coupling constant observed for these resonances was 2.6 Hz, consistent with the expected *J*-values of 2.5 Hz typically obtained for group IV metallocenes with one substituent on each ring.[21] The signals corresponding to the isopropyl protons appeared further upfield as a septet (^3J = 6.8 Hz) for the methine proton and a doublet (relative intensity 6) for the methyl protons with a common coupling constant of (^3J = 6.8 Hz). The remaining singlet corresponded to the *geminal* dimethyl groups of the bridging quaternary carbon. To distinguish between the two chemical shifts, NOE experiments (mixing time Δ_8 = 1.0 s) were performed to examine the through-space relationship of each cyclopentadienyl sector to the components of the organic substituent (Figure 3a). Correlation of the *proximal* pseudotriplet with each portion of the aliphatic tether was observed in all three cases. The intensity of the NOE cross-peak is dependent on the inverse sixth power of the distance between the two nuclei; the strength of the dipolar coupling decreased on progressing from the *geminal* dimethyl protons closest to the cyclopentadienyl fragment to the isopropyl methyl protons and finally the furthest removed methine proton.[22] Figure 3b illustrates the possible origin of these cross-peaks.

Given the more remote location of the *distal* cyclopentadienyl protons (H_d) with respect to the alkyl group, the intensity of any NOE correlation within the ancillary unit would be expected to be weaker than in the case of the correlation to the *proximal* protons. This is generally observed; cross-peaks from H_d to the *geminal* dimethyl linkage are detected, although the extent of the dipolar couplings to the isopropyl section is too small to evolve correlation in the 2D NOESY experiment. Utilizing this technique, *proximal* and *distal* cyclopen-

(19) For related syntheses, see: (a) Polo, E.; Green, M. L. H.; Benetollo, F.; Prini, G.; Sostero, S.; Traverso, O. *J. Organomet. Chem.* **1997**, *527*, 173. (b) Renault, P.; Tainturier, G.; Gautheron, B. *J. Organomet. Chem.* **1978**, *148* (1), 35.

(20) A similar approach was used in: (a) Halterman, R. L.; Volhardt, K. P. C. *Tetrahedron Lett.* **1986**, *27*, 1461. (b) Halterman, R. L.; Volhardt, K. P. C.; *Organometallics* **1988**, *7*, 883.

(21) Siemling, U.; Jutzi, P.; Neumann, B.; Stammler, H. G. *Organometallics* **1992**, *11*, 1328.

(22) (a) Kessler, H.; Gehrke, M.; Griesinger, C. *Angew. Chem., Int. Ed. Engl.* **1988**, *27*, 490. (b) Benn, R.; Gunther, H. *Ibid.* **1983**, *22*, 350. (c) Williams, D. H.; Fleming, I. In *Spectroscopic Methods in Organic Chemistry*, 4th ed.; McGraw-Hill Book Co.: London, U.K., 1989; Chapter 3, p 114. (d) Akitt, J. W. In *NMR and Chemistry, an Introduction to Modern NMR Spectroscopy*, 3rd ed.; Chapman and Hall: New York, 1992.

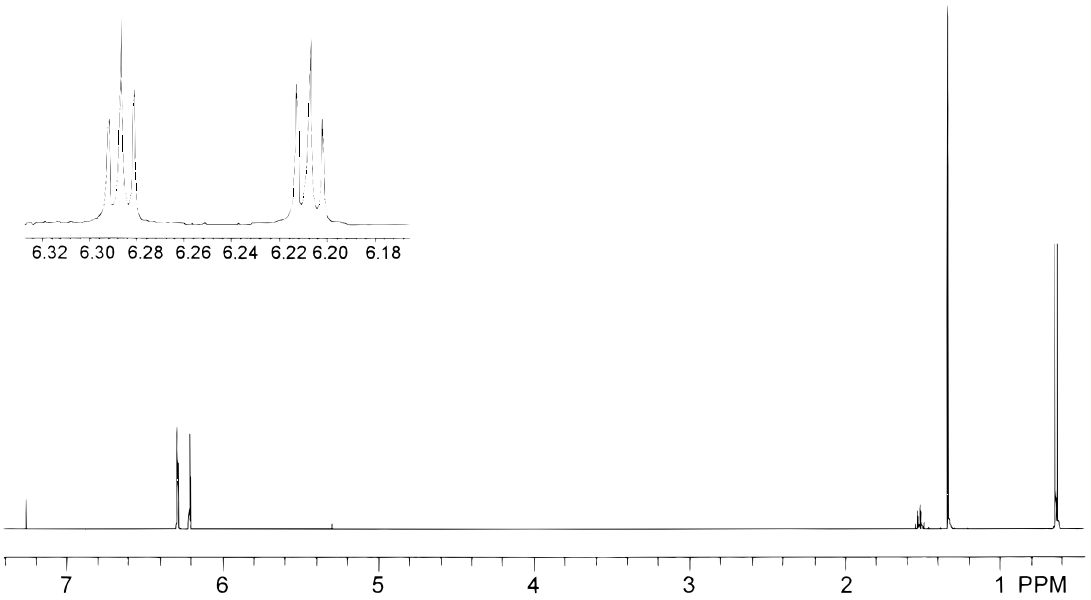

Figure 2. ^{1}H NMR of $(Cp^R)_2HfCl_2$ ($CDCl_3$, 303 K, 500 MHz).

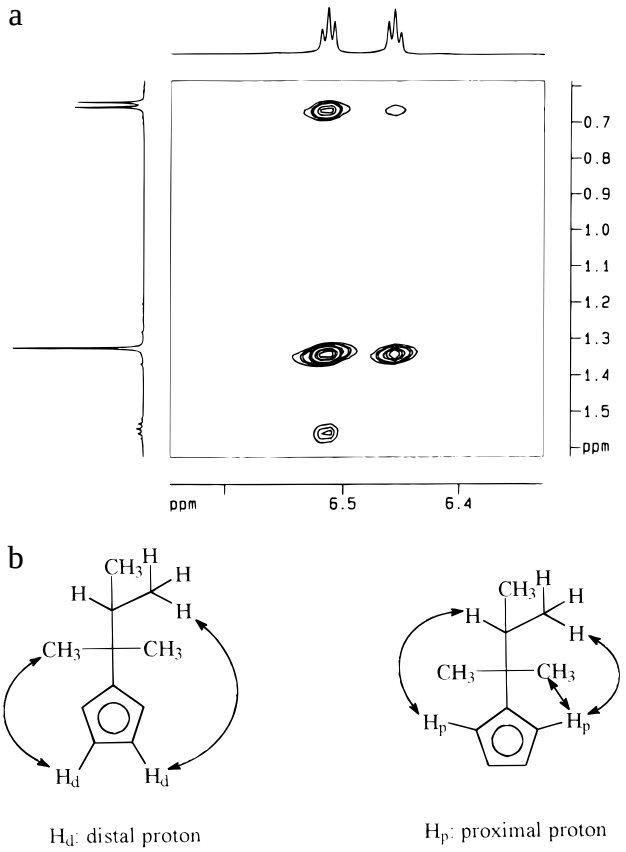

Figure 3. (a) ^{1}H−^{1}H NOESY ($CDCl_3$, 303 K, 500 MHz). The trace depicts the cross-peaks between the cyclopentadienyl region and the aliphatic region of $[C_5H_4C(Me)_2$-$CHMe_2]_2TiCl_2$ (**4**). Strong correlations from the *proximal* Cp protons (Hp) to sections of the alkyl region were observed, while only NOE contacts from the *gem*-CH_3 protons to the more remote *distal* protons H_d were obtained. (b) Possible intraligand NOE contacts between cyclopentadienyl protons H_p and H_d and *gem*-CH_3 protons.

tadienyl proton resonances were reliably assigned. A second possible mechanism for magnetization transfer between the *gem*-dimethyl protons and the H_d remains. This would involve protons from separate rings within the same molecule, assuming the dominant time average structure of the compound is that of the sterically minimized C_2 symmetric transoid form, as depicted in Figure 4 and observed in the solid-state structures. In this scenario, the inward orientation of the *gem*-CH_3 hinge toward the metal core could render those substituent protons suitably close to the *distal* protons of the neighboring ligand such that NOE communications were observed.

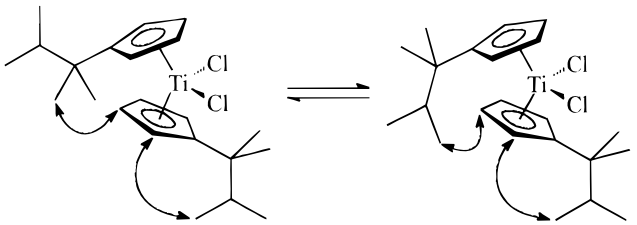

Figure 4. Possible interligand NOE contacts between cyclopentadienyl protons H_p and H_d and *gem*-CH_3 protons.

All carbon atoms were located in the $^{13}C\{^1H\}$ experiment and assigned to relevant protons signals through the HETCOR or HMQC sequences.

Solid State Analysis of Metallocenes 2−4. Crystals suitable for X-ray diffraction were obtained for all three hindered group IV metallocenes, with relevant data presented in Tables 1 and 2. The C_2 symmetric heteroannular disubstituted complexes were synthesized by various methods; however recrystallization from a chilled (0 °C) solution of CH_2Cl_2 provided isomorphous red needlelike crystals for **3** and colorless needles for **2** and **4**, which were solved in the space group *C*2/*c*. Two aspects of these structures are presented in Figures 5 and 6 for **4** and **2**, repectively. A space-filling view of **3** is shown in Figure 7.

In each case, the metal center adopts a pseudotetrahedral geometry with respect to the surrounding chloride ligands and Cp ring centroids. The cyclopentadienyl ligands were inclined in a staggered conformation, while the ring substituents were disposed in a pseudo-trans manner in order to minimize steric constraints.[19,23] This somewhat antiperiplanar geometry was highlighted in Figure 8a by the dihedral angle θ_d defined as

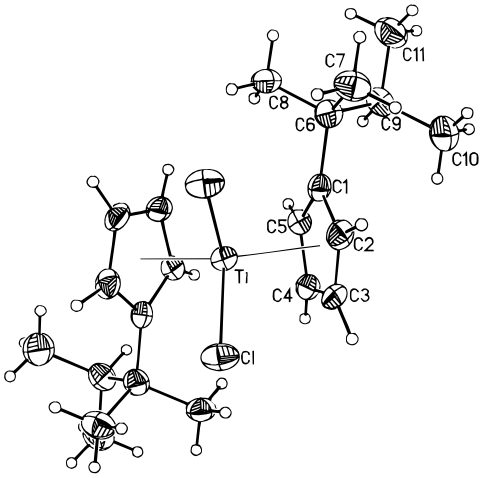

Figure 5. ORTEP plot of $(Cp^R)_2TiCl_2$ at 50% probability ellipsoids. The isopropyl sectors are positioned away from the metal center. Inward twisting the *gem*-CH_3 groups renders them in closer proximity to the *distal* protons of the neighboring Cp^R ring.

Table 2. Selected Bond Lengths (Å) and Angles (deg) for 2, 3, and 4

	Ti (**4**)	Zr (**2**)	Hf (**3**)
M−Cl(1)	2.3651(11)	2.4546(6)	2.4281(4)
M−C(1)	2.494(4)	2.600(2)	2.5906(14)
M−C(2)	2.442(4)	2.509(2)	2.4922(14)
M−C(3)	2.388(4)	2.457(2)	2.435(2)
M−C(4)	2.317(4)	2.507(2)	2.491(2)
M−C(5)	2.387(4)	2.560(2)	2.544(2)
M−X(1A)	2.086(2)	2.223	2.203(2)
C(6)−C(9)	1.574(5)	1.570(3)	1.568(2)
C(1)−C(2)	1.419(5)	1.420(3)	1.418(2)
C(2)−C(3)	1.393(5)	1.411(3)	1.419(2)
C(3)−C(4)	1.397(6)	1.402(3)	1.407(3)
C(4)−C(5)	1.404(5)	1.407(3)	1.409(3)
C(1)−C(5)	1.406(5)	1.422(3)	1.422(2)
C(1)−C(6)	1.537(5)	1.532(3)	1.530(2)
C(6)−C(8)	1.529(5)	1.535(3)	1.537(2)
C(9)−C(11)	1.526(3)	1.532(4)	1.526(2)
C(9)−C(10)	1.514(3)	1.527(4)	1.537(3)
Cl(1)−M−Cl(1′)	92.54(6)	93.95(3)	93.49(2)
C(7)−C(6)−C(8)	109.4(4)	108.9(2)	109.2(2)
C(11)−C(9)−C(10)	109.3(4)	109.4(2)	109.1(2)
C(2)−C(3)−C(4)	107.6(4)	108.8(2)	107.30(14)
C(2)−C(1)−C(5)	106.2(3)	106.5(3)	106.33(14)
X(1A)−M−X(1B)	132.4	129.4	129.8
C(1)−C(6)−C(9)	105.5(3)	106.2(4)	106.04(13)
C(1)−C(6)−C(7)	111.0(3)	110.6(2)	110.33(12)
C(4)−C(3)−C(2)	107.6(4)	108.0(3)	107.30(14)
C(5)−C(4)−C(3)	108.3(4)	108.2(3)	108.33(14)

C(6A)−X(1A)−X(1B)−C(6B) (X1A and X1B are the Cp centroids), which ranged from 170.8° to 177.0°. A perfectly trans arrangement would require $\theta_d = 180°$, indicating that the opposing centroid−alkyl vectors were moderately skewed from coplanarity. The larger isopropyl segments were fixed in an orientation directed away from the metal center, leaving the smaller methyl groups pointing into the metallocene core.

A collection of geometric parameters depicting structural aspects of the metallocenes were developed in comparison to the parent metallocenes.[23] The deviations observed are believed to occur to accommodate the bulky groups attached to the Cp ligands and are described relative to the known parent metallocenes. The parameters are illustrated in Figures 8 and presented in Table 3 and are defined as follows: D1, The tangential distance of the metal to the Cp plane; D2, distance of the normal from the metal to the plane of the cyclopentadienyl ring; Δ_S, the deviation from the Cp centroid (X1A or X1B) from the tangent of the metal to the plane of the Cp ring; Δ_R, the elevation of C(6)—the first carbon of the alkyl substituent—above the Cp plane and away from the metal center. This is described as an angular and scalar deviation; θ_d, the dihedral angle C(6A)−X(1A)−X(1B)−C(6B), which illustrates the orientation of the alkyl substituents, e.g. transoid; X1A/X1B, centroids of the cyclopentadienyl rings; α, the angle X1A−M−X1B; β, the angle Cl(1)−M−Cl(2).

For $(Cp^R)_2HfCl_2$, the average metal−C_{ring} distance (Table 1) was 2.511 Å and the Cp ring carbons remained essentially planar, deviating by 0.010 Å from the absolute planarity of a C5 ring. The Hf metal normal to the aromatic plane was not found at the centroid; rather it was located 0.148 Å further away from the *ipso* carbon C(1) with respect to X(1A). Additionally, the metal was not equidistant from the five ring carbons and two series of metal−C_{ring} distances were found: three of shorter bond lengths (2.435(2)−2.422(14) Å, an average of 2.427 Å) similar to those of Cp_2HfCl_2 (2.462−

(23) Cardin, D. J.; Lappert, M. F.; Raston, C. L. In *Chemistry of Organo-Zirconium and Organo-Hafnium Compounds*; John Wiley and Sons: New York, 1986.

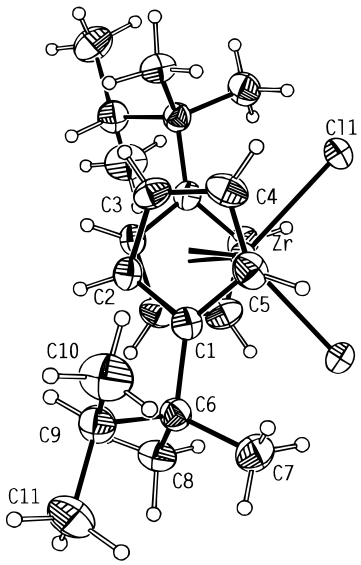

Figure 6. ORTEP plan view of the C_2 symmetric $(Cp^R)_2$-$ZrCl_2$ at 50% probability ellipsoids highlighting the trans disposition of the alkyl substituents.

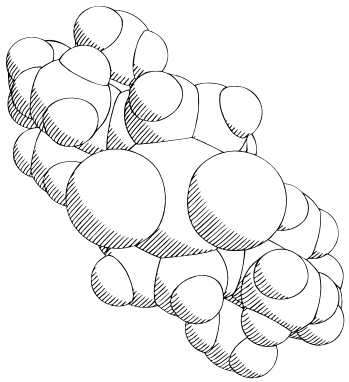

Figure 7. Space-filling model of the sterically hindered bis-substituted heteroannular metallocene (**4**).

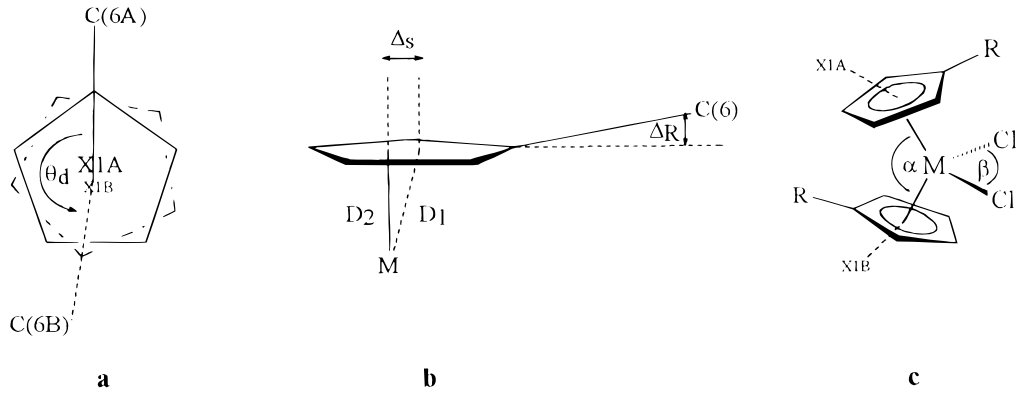

Figure 8. (a) Illustration of C(6)−X(1A)−X(1B)−C(6A) dihedral angle parameter θ_d. (b) Illustration of slippage parameter Δ_S and alkyl deviation Δ_R. (c) Illustration of metallocene angles α (X1A−M−X1B) and β (Cl−M−Cl).

Table 3. Calculated Metallocene Parameters for $(Cp^R)_2MCl_2$ [M = Ti(4), Zr (2), Hf (5)]

	Ti (4)	Zr (2)	Hf (3)
α (deg)	132.4	129.4	129.8
β (deg)	92.5	93.9	93.5
Δ_R (deg, Å)	8.9, 0.260	8.5, 0.245	8.6, 0.250
Δ_S (Å)	0.158	0.133	0.148
D_1	2.089	2.223	2.203
D_2	2.083	2.219	2.198
θ_d (deg)	172.2	170.8	177.0
X(1A)−X(1B) (Å)	3.807	4.020	3.989

2.501 Å, an average of 2.481 Å) and two significantly longer distances (2.544(2) and 2.5906(14) Å), which corresponded to the *ispo* carbon and an adjacent *proximal* Cp carbon. These two factors suggested that some degree of ring slippage occurred; the metal was displaced from the centroid position (Δ_S, Table 3) and relocated further from C(1) as a means of accommodating the steric bias associated with the pendant alkyl substituent. For the remaining congeners, **2** and **4**, similar trends were observed on evaluation of the hapticity slippage parameter (Δ_S); significantly, the largest atom, Zr, had the smallest deviation from the absolute centroids X1A/X1B, while the smallest metal, Ti, displayed the greatest extent of slippage. A related pattern was noted in the centroid−centroid gap [X(1A)−X(1B), Table 3], where the centroid span for **2** and **3** is significantly larger (3.989−4.020 Å) than the corresponding titanocene **4** (3.801 Å). This highlights the capacity of each metal to host the two isoleptic hindered ancillary ligands and minimize their mutual steric repulsion. The amount of slippage required to alleviate the steric strain caused by the alkyl substituents is smaller for the larger metals because the ligands are located further from one another.

The angle (α) subtended by the centroids at the metal centers ranged from 129.4° to 132.4° (Table 3), the deviation from perfect tetrahedral geometry being consistent with minimization of the steric environment encountered, namely, a balance between repulsions of the two Cp rings and the interaction of the alkyl chains with the metal dichloride sector at the metallocene aperture. The range of α is moderately changed for **4** but remains essentially the same for **2** and **3** in comparison to the parent $(C_5H_5)_2MCl_2$ systems (129.2−131.0°) and relates well to the data obtained for the similarly hindered compounds $(^tBuC_5H_4)_2MCl_2$ (M = Ti, Zr); α = 130.9° and 128.7°, respectively.[24a] The steric consequences causing the minor change in η^5-Cp hapticity for **2**, **3**, and **4** were accompanied by reduction of the Cl−M−Cl angles (β) to a range of 92.5° to 93.9°, which are smaller than those observed in the corresponding parent metallocenes (β = 94.5−96.2°).[24b] This contraction was an appropriate gauge of the hindered nature of heteroannular dialkyl substituted metallocenes in a d^0 configuration and was also observed for $(^tBuC_5H_4)_2MCl_2$ (M = Ti, Zr), where similar data of 92.5° and 94.3°, respectively, were obtained for β. Generally, the alkyl moieties encroached the chloride coordination sphere, which induced a closure in β to control repulsions between the halogens and the approaching methyl substituents. This compensation to accommodate the bulky alkyl groups can be further exemplified on consideration of Hf compound (**3**); the chloride−*gem*-$(CH_3)_2$ nonbonded distance [Cl···C(7), Cl···C(8)] was noticeably extended to an average of 3.696 Å without significant alteration of the position of the Cp centroid from the metal site, with α = 129.8°. The centroid distance X(1A)−X(1B) was maintained at 3.989 Å, which is close to that of Cp_2HfCl_2 (129.2°, 3.939 Å). Furthermore, a deviation of the C(1)−C(6) bond (*ipso*C−*quaternary*C) from coplanarity by 8.8° and 0.250 Å with respect to the mean plane of the Cp aromatic ring also extended the quaternary alkyl carbon−chloride nonbonded distance [Cl···C(6)] to 3.779 Å and demonstrated the molecular rearrangements to minimize spatial conflicts. In tandem, the β angle was reduced to 93.5° to reduce the spatial conflict. The deflection of the C(1)−C(6) vector from the aromatic plane Δ_R was also observed for **2** and **4**; the data are presented in Table 3.

All atoms, including hydrogen atoms, were located and all three structures refined anisotropically to yield accurate hydrogen bond distances and permit relevant discussion of important H−H nonbonded distances listed in Table 4. Two types of bond distances were examined.

1. The distance between each *distal* Cp proton H(3)/H(4) and all *geminal* methyl protons of the same cyclopentadienyl ligand H(7)/H(8). The average intramolecular nonbonded distances were then also calculated for H_d−(*gem*-CH_3).

(24) (a) Howie, R. A.; McQuillan, G. P.; Thompson, D. W.; Lock, G. A. *J. Organomet. Chem.* **1986**, *303*, 213. (b) Cp_2TiCl_2: Clearfield, A.; Warner, D. K.; Saldarriga-Molina, C. H.; Ropal, R.; Bernal, I. *Can. J. Chem.* **1975**, *53*, 1622. Cp_2ZrCl_2: Corey, J. Y.; Zhu, X.-H.; Brammer, L.; Rath, N. P. *Acta Crystallogr. Sect. C* **1995**, *51*, 565. Cp_2HfCl_2: Soloveichik, G. L.; Arkhiveera, T. M. Bel'skii, V. K.; Bulychev, B. M. *Metalloorg. Khim.* **1988**, *1*, 226.

Table 4. Calculated Intra-[a] and Intergeminal Dimethyl−Distal Cp H···H Nonbonded Distances (Å)

	Ti		Zr		Hf	
	H(**3**)[a]	H(**4**)[a]	H(**3**)[a]	H(**4**)[a]	H(**3**)[a]	H(**4**)[a]
H(7A1)[b]	4.867	5.663	5.769	4.948	6.197	6.571
H(7B1)	5.026	5.707	5.645	4.734	5.385	5.645
H(7C1)	6.098	6.470	6.409	5.903	4.939	5.805
H(8A1)[b]	6.546	6.021	5.445	6.095	5.860	6.060
H(8B1)	5.601	5.168	5.766	6.387	6.600	4.790
H(8C1)	5.864	4.838	4.942	5.107	5.735	5.029
H(av)[d]	*5.667*	*5.645*	*5.663*	*5.529*	*5.786*	*5.650*
H(7A2)[c]	6.117	5.618	4.901	5.767	3.805	4.991
H(7B2)	4.867	4.828	5.247	5.519	2.792	3.538
H(7C2)	5.954	5.444	6.137	6.503	2.525	4.332
H(8A2)[c]	4.761	3.742	3.772	4.907	5.626	6.624
H(8B2)	3.199	3.742	2.713	3.481	5.897	6.510
H(8C2)	4.246	2.612	2.510	4.287	5.038	5.210
H(av)[e]	*4.857*	*4.331*	*4.215*	*5.077*	*4.311*	*5.200*

[a] H(3) and H(4) entries correspond to located H_d protons. [b] H(7:1)−H(8:1) denote interligand (*gem*-CH_3) protons; the entries show calculated H···H nonbonded distances with respect to the *distal* protons. [c] H(7:2)−H(8:2) denote intraligand (*gem*-CH_3) protons; the entries show calculated H···H nonbonded distances with respect to the *distal* protons. [d] Average intraligand H_d−(*gem*-CH_3) proton nonbonded distance. [e] Average interligand H_d−(*gem*-CH_3) proton nonbonded distance.

2. The distance between the *distal* Cp protons of one ring and the *geminal* methyl protons of the second ring, H(3)−H(7′). The average intermolecular nonbonded distances were then also calculated.

For all three structures, the average distance from the *distal* protons H(3)/H(4) of one ring to the *gem*-CH_3 protons of the neighboring ancillary ligand H(7:2)/H(8:2) of 4.594−4.756 Å was actually significantly shorter than the corresponding average internal ligand distance (5.596−5.718 Å). Therefore the solid-state structure suggested that the H_d and *gem*-CH_3 groups located on opposing rings were consistently about 1 Å closer; implying that the steric and electronic environment of H_d was dependent more on interligand alkyl contact in the same molecule rather than intraligand interaction.

Solution Studies of Monosubstituted Metallocenes $Cp(Cp^R)MCl_2$. For the monosubstituted metallocene dichlorides $CpCp^RMCl_2$ (M = Ti [**5**], Zr [**6**]) similar NMR studies were also undertaken which further supported the origin of the NOEs concerning the *distal* Cp protons. The ^1H NMR resonances for the alkyl-substituted cyclopentadienyl ligand adopted the same multiplicities and chemical shift pattern as seen with the corresponding $(Cp^R)_2MCl_2$ metallocene. In addition, a singlet (relative intensity 5) was observed in the cyclopentadienyl region representing the unsubstituted Cp ring. NOESY spectroscopy (Figure 9) indicated a correlation between all protons of the alkyl substituent and the *proximal* Cp^R protons (H_p) of the aromatic ring. In contrast to the heteroannular disubstituted species, no cross-peaks were observed between the *distal* protons (H_d) and the alkyl substituent, which suggested that the distance between the two groups precludes intraligand dipolar coupling. Additionally, NOEs arising from the equivalent Cp protons externally to the *geminal* dimethyl protons of the neighboring Cp^R ligand were observed. Thus, the distance between H_d and *geminal* dimethyl protons (*gem*-CH_3) is larger than that between the unsubstituted ring and the *geminal* dimethyl protons such that NOE was only observed in the latter case.

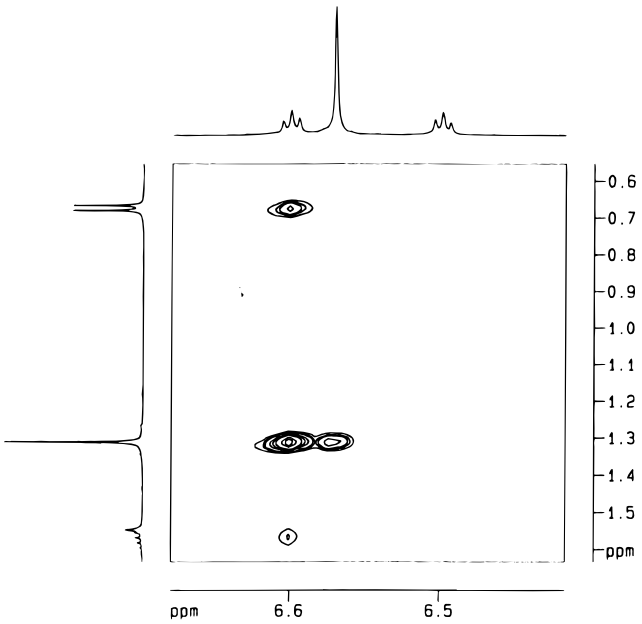

Figure 9. $^1H-^1H$ NOESY ($CDCl_3$, 303 K, 500 MHz). The trace depicts the cross-peaks between the cyclopentadienyl region and the aliphatic region of $Cp(C_5H_4C(Me)_2CHMe_2)TiCl_2$ where only NOEs between H_p and *gem*-CH_3 groups were obtained. NOE contacts between H_d and the unsubstituted Cp protons were also observed, suggesting an interligand mechanism for the H_d to *gem*-CH_3 NOE observed in the upper spectrum.

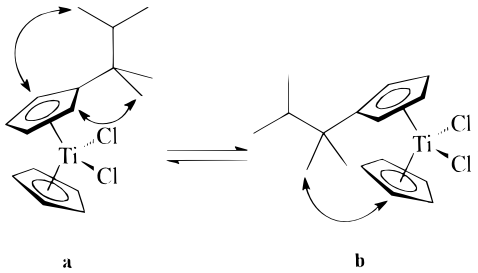

Figure 10. Proposed interligand NOE contacts between cyclopentadienyl protons H_d and *gem*-CH_3 protons for monosubstituted titanocene **6**. The conformer with the pendant alkyl substituent directed away from the metal core allows NOE to H_p protons of the same ring. The NOE contacts observed between the *gem*-CH_3 groups and the C_5H_5 ring imply that rotation of the Cp^R ring must occur to permit this interaction.

Similar structural features of other Cp-based systems in solution have been determined using NOE effects.[25] This demonstrates that the η^5-Cp^R ligand rotates in solution to establish NOE contacts not only between the C_5H_5 protons and the H_d protons of the substituted ring but also between the C_5H_5 and the *gem*-CH_3 species. Although the X-ray structure of **6** indicates the sterically minimized rotamer (a in Figure 10) exists in the solid state (vide supra), there must exist a second state (b in Figure 10) in which the C_5H_4R substituent has effectively rotated 180° to allow NOE between the *gem*-

(25) (a) Okuda, J.; Verch, S.; Spaniol, T. P.; Sturmer, R. *Chem. Ber.* **1996**, *129*, 1429. (b) Mitani, M.; Hayakawo, M.; Yamada, T.; Mukaiyama, T. *Bull. Chem. Soc. Jpn.* **1996**, *69*, 2967. (c) Burckhardt, U.; Gramlich, V.; Hofmann, P.; Reinhard, N.; Pregosin, P. S.; Salzmann, R.; Togni, A. *Organometallics* **1996**, *15*, 3496. (d) Togni, A.; Burckhardt, U.; Gramlich, V.; Pregosin, P. S.; Salzmann, R. *J. Am. Chem. Soc.* **1996**, *118*, 1031.

CH_3 and C_5H_5 protons (Figure 10). This also implies that for metallocenes **2**−**4**, $(Cp^R)_2MCl_2$, the NOE between *distal* Cp^R protons and the alkyl substituent occurred by an interligand mechanism; that is, NOE contacts from (*gem*-CH_3) protons of one ring to the H_d protons of the second ring are stronger because the distance in solution is closer than the H_d−(*gem*-CH_3) within the same ancillary ligand (Figure 3). Variable-temperature studies of the disubstituted metallocene **4** in toluene-d_8 did not produce noticeable line-broadening effects before precipitation of the compound (−70 °C). Elevated temperatures (up to 105 °C) failed to produce line-broadening effects, which would be expected if the metallocene framework was static at lower temperatures. This suggested that any motion of **4** was too rapid to be significantly slowed at this temperature limit or that there was no perceptible change in rotation of the substituted rings. Although the temperature threshold of the ring dynamics falls ouside the temperature limits investigated, literature precedents favor at least partial rotation or a rocking motion of the substituted rings.[26]

Red needles of **6** were obtained by recrystallization from $CHCl_3$ and studied by X-ray diffraction. However, the quality of the crystals was poor, and only atomic connectivity could be reliably determined. Attempts to obtain a suitable sample for crystallographic studies are in progress in order to assess relevant H−H nonbonded distances.

Conclusions

A series of sterically hindered monosubstituted and heteroannular disubstituted group IV metallocenes **2**−**6** were synthesized by traditional salt metathesis procedures and characterized by a combination of NMR spectroscopy and X-ray crystallography. The complexes $(Cp^R)_2MCl_2$ adopt a C_2 symmetric geometry with a transoid conformation of the alkyl substituents in the solid state. Examination of the structural parameters of **2**−**4** with reference to the parent metallocenes and related substituted species showed that some important architectural modifications were made to minimize the steric situation presented by the incumbent alkyl substituents.

Consolidation of selected nonbonded H−H distances with observed $^1H-^1H$ NOE signals led to the conclusion that a related modified C_2 symmetric structure for **2**, **3**, and **4** was present as a time-averaged structure in solution. Given the size of the ring substituents, there is an onus for hindered rotation as a pendant rocking motion of the aromatic ligands. It is probable that the ligands engage in some rotational motion and deviate substantially from C_2 symmetry. However, given the NOE characteristics of these compounds, it is also likely that the "center of gravity" for this motion lies close to or at the C_2 geometry. The consequence of this hindering motif as a modification to the ancillary ligand is that it not only enforces adjustments in the π-bonding of the Cp housing to the metal center but also serves to tighten the metallocene framework. This could be reasonably expected to adjust the reactivity of the metal center with respect to approaching substrates; that is the alkyl groups impinge on the metal coordination sphere and retard the advance of larger reactants or dictate their particular routes and orientations in order to access the metal site. The monosubstituted metallocenes appear to engage in full rotation of the substituted and nonsubstituted rings; otherwise the NOE obtained between the *gem*-CH_3 and C_5H_5 protons would not be feasible. The testing of the metallocene reactivity with regard to dehydropolymerization of silanes to polysilanes will be described in a subsequent paper.

Acknowledgment. Funding from the NSF, U.M. Research Board, U.M. Graduate School, and Mallinckrodt Foundation for B.G. is gratefully acknowledged. We also thank Prof. C. D. Spilling and Dr. J. Braddock-Wilking for helpful discussions, J. C. Mareque-Rivas for assistance in the structure determination of **2**, and Q. Wang for assistance in the synthesis of **4**.

Supporting Information Available: Tables of crystal structure data and refinement details, atomic coordinates and equivalent isotropic displacement parameters, and hydrogen coordinates and isotropic displacement parameters for **2**−**4**. This material is available free of charge via the Internet at http://pubs.acs.org.

OM9808615

(26) (a) Thiele, H.-H.; Bohme, U.; Peters, K.; Peters, E.-M.; Walz, L.; von Schnering, H. G. *Z. Anorg. Allg. Chem.* **1993**, 771. (b) Winter, C. H.; Zhou, X. X.; Hegg, M. J. *Inorg. Chem.* **1992**, *31*, 1808. (c) Choukroun, R.; Dahan, F. *Organometallics* **1994**, *13*, 2097.